Journal of NUCLEAR SCIENCE and TECHNOLOGY, Supplement 1, p. 258–262 (March 2000)

Monte Carlo Analyses for ITER NBI Duct by 1/4 Tokamak Model

Satoshi Sato*,† and Hiromasa Iida*

Japan Atomic Energy Research Institute

In the ITER shielding design, the biological dose rates after shutdown in the region around the NBI ducts are critical. We have performed shielding calculations for the ITER/NBI ducts by 3-D Monte Carlo and 2-D SN codes with activation calculations. From comparison between calculated results by 3-D Monte Carlo and 2-D SN calculations, it has been found that the calculated results by the 2-D SN calculation overestimate by a factor of about eight at the cryostat in the case of the 91.5 cm high duct opening. From the 2-D SN calculation with activation calculations, we have deduced the conversion ratio relating fast neutron flux to the biological dose rates of ~ 1.5 - 2.0 x 10^{-5} μSv/hour/(cm^{-2}sec.$^{-1}$). The biological dose rates are about 7 x 10 μSv/hour in 50 – 60 cm thick duct wall from the fast neutron flux by the 3-D Monte Carlo calculation and the conversion ratio, and they can satisfy the design criteria.

KEYWORDS: ITER, NBI duct, shielding design, 3-D Monte Carlo calculation, 2-D SN calculation, activation calculation, biological dose rates, neutron streaming, calculated error, variance reduction

I. Introduction

In the International Thermonuclear Experimental Reactor (ITER) Engineering Design Activity (EDA), Neutral Beam Injection (NBI) ducts[1, 2] are located in the confined space between adjacent Toroidal Field (TF) coils. Plasma heating is accomplished with three NBI ducts that enter the plasma region tangent to the plasma axis at R = 6.5 m. The NBI ducts are completely open (91.5 cm high by 58 cm wide at the plasma facing region) to allow direct injection of deuterons into the plasma. Consequently, the inner surfaces of the NBI ducts will be highly activated. Because of space limitation due to the reactor configuration, the shielding thickness of the NBI ducts is restricted. In the midplane ducts except for the NBI ducts, shield plugs can be installed in plasma facing regions to reduce the radiation streaming through the midplane ducts. Shield plugs, however, can not be installed in the NBI ducts. At the cryostat, human access for hands-on maintenance is required. The biological dose rates after shutdown around the NBI ducts may possibly be much higher than the design criteria of 100 μSv/hour required for human access at the cryostat. Thus, the biological dose rates after shutdown in the region around the NBI ducts are critical, and we have performed shielding calculations for the ITER NBI ducts using 3-D Monte Carlo and 2-D discrete ordinates SN methods with activation calculation.

In the ITER Conceptual Design Activity (CDA), shielding calculations for the ITER NBI ducts had been performed using 2-D SN calculations[3,4] since it had been expected that it was very time-consuming to perform shielding calculations for the ITER NBI ducts by a 3-D Monte Carlo calculation. However, it has been expected that calculated results by 2-D SN calculations enormously overestimate because the infinite continuous opening of the NBI duct is assumed in the Z direction. So we have performed 3-D Monte Carlo and 2-D SN calculations, and we have evaluated calculated error for 2-D SN calculations. In addition to the calculation for the model with the 91.5 cm high duct opening which is a reference design, we have performed 3-D Monte Calro calculations for the models with 5 - 158 cm high duct openings and we have evaluated calculated errors for each model.

We have calculated fast neutron flux (> 0.1 MeV) distributions in the region between adjacent two NBI ducts by a 3-D Monte Calro calculation with variance reduction techniques that can reduce calculation time drastically. Also, we have calculated operational fast neutron flux and shutdown gamma-ray biological dose rate distributions by 2-D SN calculations with activation calculations. From the results, we have evaluated the conversion ratio relating fast neutron flux to the biological dose rates. In this study, we have evaluated the biological dose rates in the region between adjacent two NBI ducts using conversion ratios obtained from 2-D SN/activation calculations and the fast neutron flux obtained from 3-D Monte Carlo calculations.

II. Calculation Methods and Models

We have performed 3-D shielding calculations using the Monte Carlo Neutron and Photon transport code MCNP-4A[5] with the Fusion Evaluated Nuclear Data Library FENDL-1[6]. We have performed calculations for two NBI duct configurations. A vertical cross section view of the calculation models is shown in **Fig. 1**, and horizontal cross section views are shown in **Figs. 2** and **3**. The models represent 1/4 (90°) tokamak device, and they include all of the main tokamak components, such as the blanket modules, vacuum vessel, divertor cassettes, cryostat, biological shield, Toroidal Field (TF) coils, Poloidal Field (PF) coils, three NBI and two standard equatorial ducts, and five divertor and upper ducts. NBI duct walls are 40 - 43 cm in thickness in the calculation model shown in Fig. 2, and they are 50 - 60 cm in thickness in that in Fig. 3. We have modeled 14 MeV neutron source in the plasma region shown

* *Naka-machi, Naka-gun, Ibaraki-ken 311-0193*
† Corresponding author, Tel. +81-29-270-7583,
Fax. +81-29-270-7539, E-mail: sato@naka.jaeri.go.jp

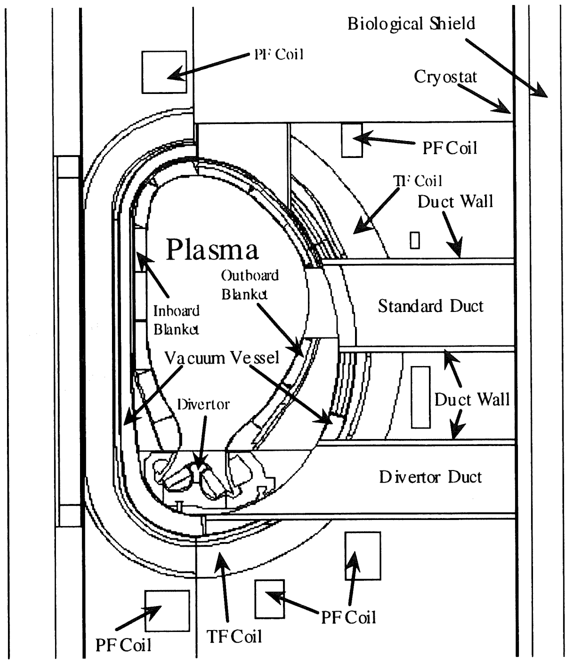

Fig. 1 Vertical cross section view of MCNP model

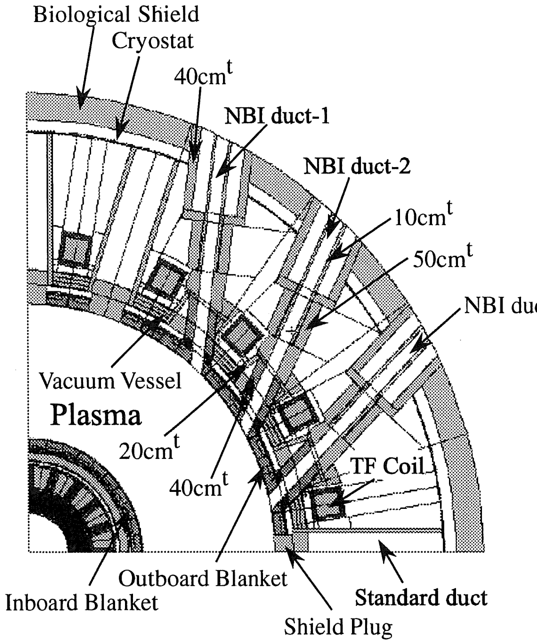

Fig. 3 Horizontal cross section view of MCNP model

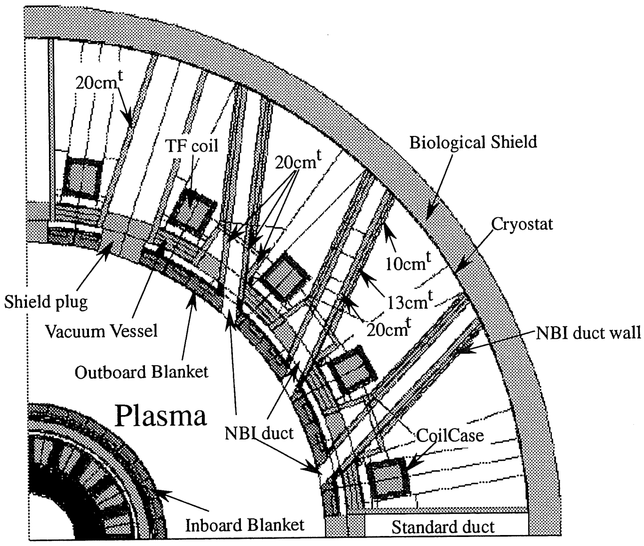

Fig. 2 Horizontal cross section view of MCNP model

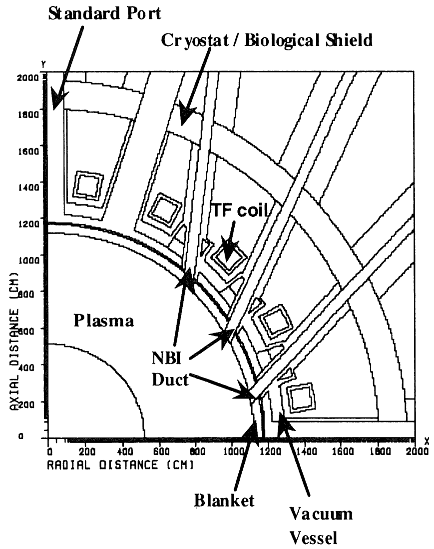

Fig. 4 XY model for 2-D SN DOT calculation

in Figs. 1 - 3 according to the fusion reaction distribution at 1.5 GW fusion power. Also, we have performed 2-D shielding calculations using the SN code DOT3.5[7] with nuclear group constant set based on FENDL-1 and the activation calculation code CINAC-V4[8].

1. Comparison of the Calculated Results between 3-D Monte Carlo and 2-D SN Methods

We have estimated fast neutron flux distributions with energy above 0.1 MeV in the NBI duct by MCNP with the model shown in Fig. 2 and DOT with the 2-D calculation model shown in **Fig. 4**. We have compared the calculated results, and we have estimated the calculated errors for 2-D calculation. We have performed 3-D calculations for the duct openings with 5, 10, 15, 30, 60, 91.5, 120 and 158 cm height, and we have estimated calculated errors for the 2-D calculation as well as neutron flux distributions in NBI ducts for each duct opening. We have used point detectors[5] with 1, 2, 3 and 6 cm in radius for the models with 5, 10, 15 and 30 - 158 cm high duct openings, respectively, in the 3-D Monte Carlo calculations, and we have estimated the neutron fluxes with statistical fluctuation of less than 5 %. As the duct openings are higher, we use the point detectors with larger radius in order to reduce the calculation time.

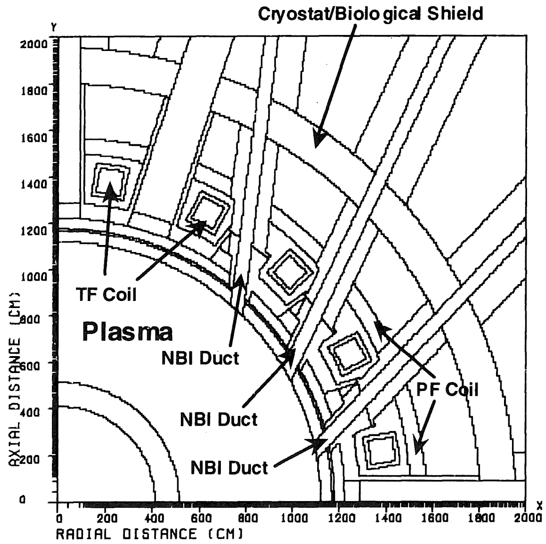

Fig. 5 XY model for 2-D SN DOT calculation

2. Evaluation of the Fast Neutron Flux and Dose Rate

Using the 2-D calculation model shown in **Fig. 5**, we have estimated distributions of fast neutron flux with energy above 0.1 MeV and the gamma-ray biological dose rates in 10^6 seconds after reactor shutdown by 2D SN calculations with activation calculation[(9)(10)]. The activation calculation has been performed based on the ITER operation scenario[(10)] to estimate the residual gamma-ray source in 10^6 seconds after shutdown. From the results, we have estimated conversion ratios relating fast neutron flux to the biological dose rates.

In 3-D Monte Carlo calculations, we have estimated average fast neutron flux in the regions between adjacent two NBI ducts using the track length estimator[(5)]. We have used the weight window table as well as the energy cut-off of 0.1 MeV as variance reduction techniques to reduce the calculation time in the Monte Carlo calculation[(5)(10)]. In order to set more effective weight window tables in the Monte Carlo calculation for the model with 50 – 60 cm thick duct wall shown in Fig. 3, we have performed the neutron streaming calculations from each NBI duct independently by separate two calculations[(10)]. Finally, we have estimated the fast neutron flux in the region between adjacent two NBI ducts by summing the results obtained by each calculation. We have estimated statistical fluctuations for the estimated fast neutron flux between NBI duct-1 and duct-2 using the following formula

$$\delta = \frac{\sqrt{(m_1 \times \delta_1)^2 + (m_2 \times \delta_2)^2}}{m_1 + m_2} ,$$

where δ is a total statistical fluctuation, m_1 and m_2 are mean values of the fast neutron flux from the NBI duct-1 and duct-2, respectively, δ_1 and δ_2 are statistical fluctuations for m_1 and m_2, respectively. From conversion ratios by the 2D SN calculations with activation calculation and fast neutron flux by the 3D Monte Carlo calculations, we have estimated the gamma-ray biological dose rates at 10^6 seconds after reactor shutdown in the regions between adjacent two NBI ducts.

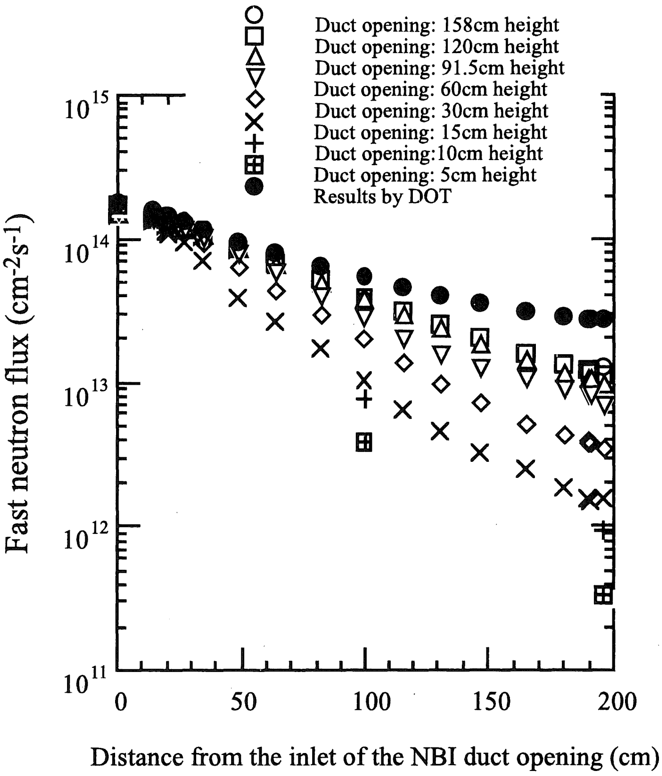

Fig. 6 Fast neutron flux distributions along the center axis in the NBI duct

III. Results and Discussion

1. Comparison of Calculated Results

Fast neutron flux distributions along the center axis in the NBI duct are shown in **Figs. 6** and 7. We have evaluated calculated errors for the 2D SN calculation using the following formula;

$$E = \frac{C_{2D}(x)/C_{2D}(0)}{C_{3D}(x)/C_{3D}(0)} ,$$

where E is a calculated error for the 2-D SN calculation, $C_{2D}(x)$ and $C_{2D}(0)$ are a calculated result at x cm distance from the inlet of the duct opening at the plasma facing region and that at the inlet by the 2-D SN calculation, respectively, $C_{3D}(x)$ and $C_{3D}(0)$ are calculated results by the 3-D Monte Carlo calculation. Estimated calculated errors are shown in **Fig. 8**. As the duct openings are lower, calculated errors for the 2-D SN calculation are bigger though it is seen that some curves are not smooth due to effect of complex configuration and statistical error of Monte Carlo calculation. In the case of 91.5 cm high opening, it has been found that the 2-D SN calculation overestimates fast neutron fluxes by a factor of about eight at the cryostat. So it can be concluded that 3-D Monte Carlo calculation are required for the shielding calculation around the NBI duct.

2. Fast Neutron Flux and Dose Rate

Contours of the conversion ratio relating fast neutron flux to biological dose rate are shown in **Fig. 9**. It has been found

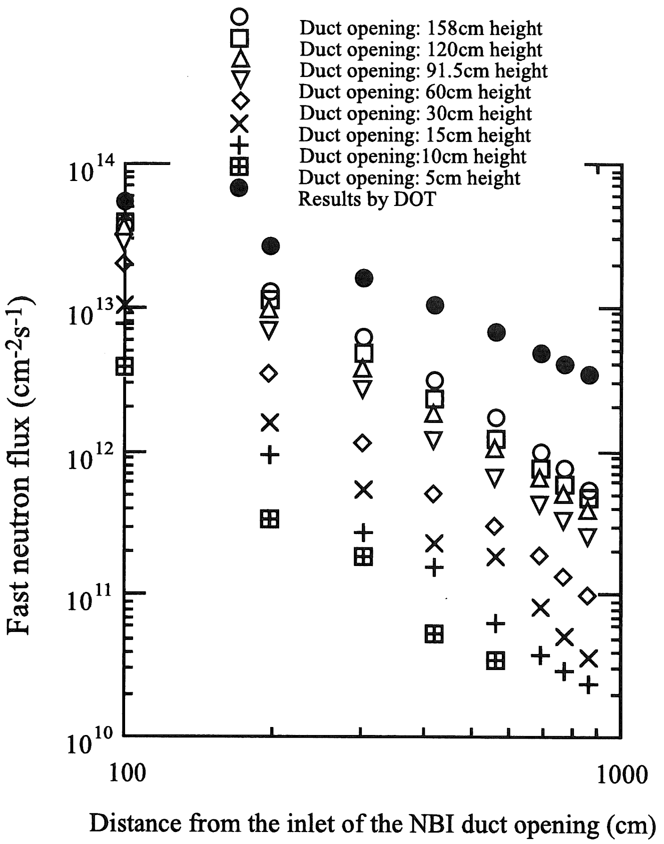

Fig. 7 Fast neutron flux distributions along the center axis in the NBI duct

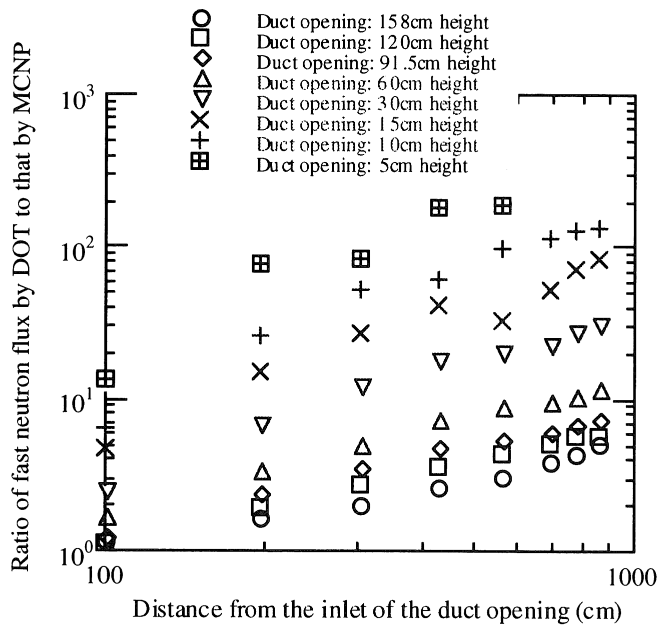

Fig. 8 Estimated calculated error for the 2-D SN calculation

that the conversion ratios are ~ 1.5 - 2.0 x 10^{-5} μSv/hour/($cm^{-2}sec.^{-1}$).

For the duct with 91.5 cm high opening, fast neutron flux distributions estimated using MCNP are shown with statistical fluctuation in **Figs. 10** and **11** for the thin (40 – 43 cm in thickness) and thick (50 – 60 cm in thickness) walled cases, respectively. The fast neutron flux is about 3.4 x 10^8 $cm^{-2}sec.^{-1}$ at the cryostat for the thin walled case, and 3.6 x 10^6 $cm^{-2}sec.^{-1}$ for the thick walled case. Using the conversion ratio of 2.0 x 10^{-5} μSv/hour/($cm^{-2}sec.^{-1}$) which is conservative, the biological dose rates at 10^6 seconds after shutdown have been estimated. The biological dose rates are shown in **Fig. 12** for the thick walled case. They are approximately 7 x 10^3 and 7 x 10 μSv/hour at the cryostat for the thin and thick walled cases, respectively. In the thick walled case, the biological dose rates can satisfy the

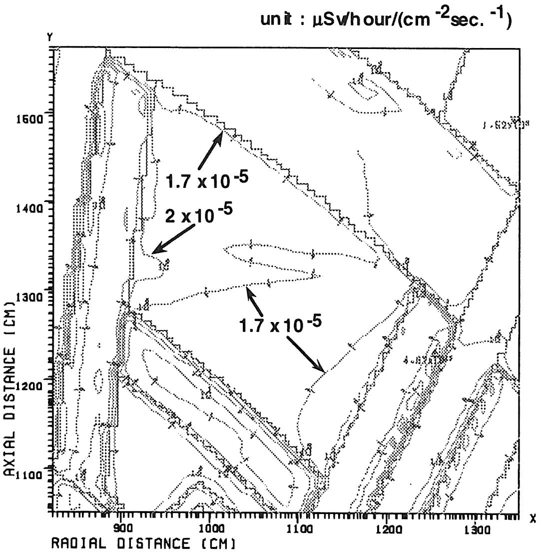

Fig. 9 Contours of the conversion ratio relating fast neutron flux to biological dose rate

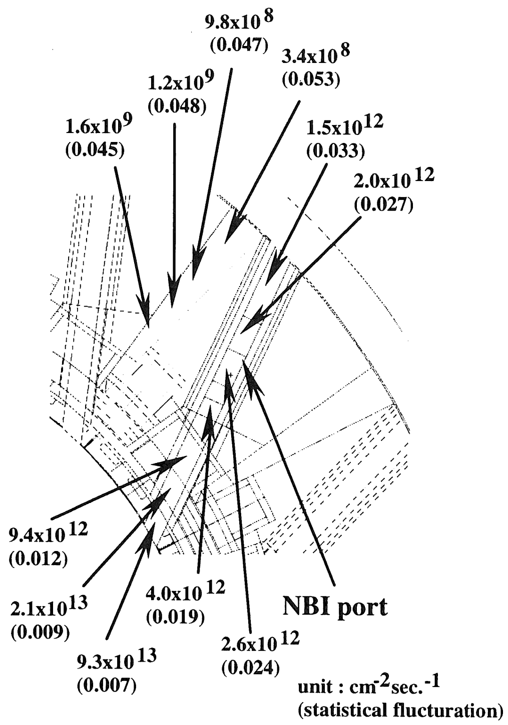

Fig. 10 Fast neutron flux distributions for the thin (40 – 43 cm in thickness) walled case

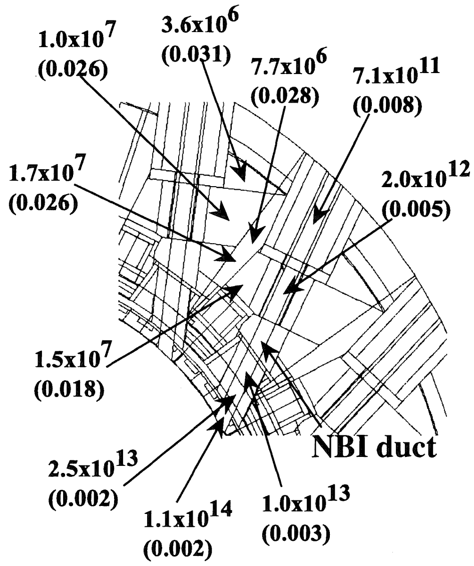

Fig. 11 Fast neutron flux distributions for the thick (50 – 60 cm in thickness) walled case

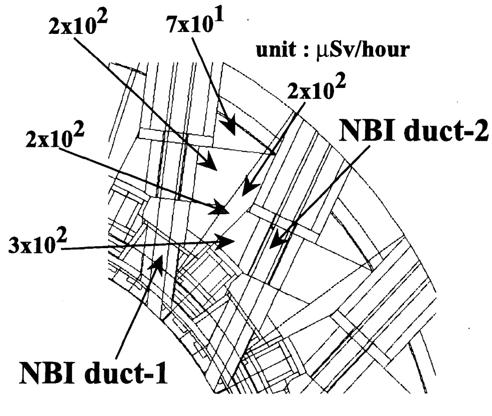

Fig. 12 Biological dose rates at 10^6 seconds after shutdown for the thick (50 – 60 cm in thickness) walled case

tentative ITER EDA design criteria of 100 μSv though a safety factor is not considered. In case a safety factor is considered, 60 – 65 cm thick duct walls are required to satisfy the tentative ITER EDA design criteria [10].

IV. Conclusion

We have performed shielding calculations for ITER NBI duct by 3-D Monte Carlo and 2-D SN methods. In addition to the calculations of the reference model with 91.5 cm high duct opening, we have performed 3-D Monte Carlo calculations for the models of the NBI duct opening with 5 - 158 cm heights. From the comparison between results by 3-D Monte Carlo and 2-D SN calculations, we have clarified the calculated error for 2-D SN calculation due to modeling. In the case of ITER reference model, the calculated error is a factor of about eight at the cryostat for fast neutron flux in the NBI duct. From fast neutron flux and shutdown gamma-ray biological dose rates distributions, we have deduced a conversion ratio of $1.5 - 2 \times 10^{-5}$ μSv/hour/(cm^{-2}sec^{-1}) at the region between adjacent two NBI ducts. In the case of 50 – 60 cm thick duct wall, the shutdown gamma-ray biological dose rates estimated from 3-D Monte Carlo calculation and the conversion ratio can satisfy the design criteria.

Acknowledgment

The authors wish to thank Drs. S. Matsuda, Y. Ohara, H. Takatsu, K. Maki, T. Inoue, K. Yamada and T. Utsumi for valuable discussions and comments.

-References-

(1) Inoue, T., *et al.* : "Design and R&D of high power negative ion source/accelerator for ITER NBI", *Proc. 19th Symp. on Fusion Technol.*, Lisbon, Portugal, Sep. 16-20, 1996, p. 701, Portugal (1996).
(2) Krylov, A., *et al.* : "General design of the neutral beam injection system and integration with ITER", *Proc. 19th Symp. on Fusion Technol.*, Lisbon, Portugal, Sep. 16-20, 1996, p. 697, Portugal (1996).
(3) Maki, K. : *Fusion Eng. Des.*, **22**, 427 (1993).
(4) Maki, K. : *Fusion Eng. Des.*, **24**, 315 (1994).
(5) Briesmeister, J. F. : "MCNP 4A Monte Carlo N-Particle Transport Code System", Oak Ridge National Laboratory, RSICC Computer Code Collection (1995).
(6) Ganesan, S., McLaughlin, P. K. : "FENDL/E, Evaluated Nuclear Data Library of Neutron Interaction Cross Sections, Photon Production Cross Sections and Photon-Atom Interaction Cross Sections for Fusion Applications, Version 1.1 of November 1994," *IAEA(NDS)*-128, Rev. 3, International Atomic Energy Agency, 1996.
(7) Rhoades, W. A., Mynatt, F. R. : "The DOT-III two dimensional discrete ordinates transport code", *ORNL-TM*-4280 (1973).
(8) Fukumoto, H. : *J. Nucl. Sci. Tecnol.* **23**, 97 (1986).
(9) Sato, S., *et al.* : *Fusion Technology*, **34**, 100 (1998).
(10) Sato, S., *et al.* : *Fusion Eng. Des.*, (in printing).